Transactions of the 17th International Conference on Structural Mechanics in Reactor Technology (SMiRT 17)
Prague, Czech Republic, August 17 –22, 2003
Paper # D03-3

Crack Growth Behavior of Irradiated Austenitic Stainless Steels in BWR Environments

O. K. Chopra,[1] E. E. Gruber,[1] W. J. Shack,[1] and J. Muscara[2]

[1)] Energy Technology Division, Argonne National Laboratory
9700 South Cass Avenue, Argonne, Illinois 60439 USA
[2)] Office of Nuclear Regulatory Research,
U.S. Nuclear Regulatory Commission, Washington, DC 20555

ABSTRACT

Crack growth tests have been performed in boiling water reactor (BWR) environments on Types 304 and 316 stainless steel that were irradiated to fluence levels up to 2.0 x 10^{21} n cm^{-2} (E > 1 MeV) at ≈288°C in a helium environment. Two waveforms were used in the tests, slow/fast sawtooth and trapezoidal. The cyclic loading was done with rise times between 30 and 1000 s. At the longer rise times, the environmental contributions to the crack growth rate dominate. The trapezoidal waveform essentially represents constant load with periodic unloading and loading. The results indicate significant enhancement of crack growth rates of the irradiated steel in the BWR environment with normal water chemistry. The effects of fluence and hydrogen water chemistry are presented.

INTRODUCTION

Austenitic stainless steels (SSs) are used extensively as structural alloys in reactor–pressure–vessel internal components because of their high strength, ductility, and fracture toughness. However, exposure to neutron irradiation for extended periods changes the microstructure and degrades the fracture properties of these steels. Irradiation leads to a significant increase in yield strength and reduction in ductility and fracture resistance of austenitic SSs [1–4]. Radiation can exacerbate the corrosion fatigue and stress corrosion cracking (SCC) of SSs [1,5,6] by affecting the material microchemistry, for example, radiation–induced segregation; material microstructure, e.g., radiation hardening; and water chemistry, e.g., radiolysis.

The factors that influence SCC susceptibility of materials include neutron fluence, cold work, corrosion potential, water purity, temperature, and loading. The effects of neutron fluence on irradiation–assisted stress corrosion cracking (IASCC) of austenitic SSs have been investigated for BWR control blade sheaths [7,8] and laboratory tests on BWR–irradiated material [5,9–11]; the extent of intergranular SCC increases with fluence. Although a threshold fluence level of 5 x 10^{20} n/cm^2 (E >1 MeV) has been reported for austenitic SSs in the BWR environment, experimental data show an increase in intergranular cracking above a fluence of ≈2 x 10^{20} n/cm^2 (E >1 MeV) (≈0.3 dpa). The results also show the beneficial effect of reducing the corrosion potential of the environment [12,13]. However, low corrosion potential does not provide immunity to IASCC, e.g., intergranular SCC has been observed in cold–worked, irradiated SS baffle bolts in pressurized water reactors (PWRs). The threshold fluence for IASCC is higher under low potential conditions such as hydrogen water chemistry (HWC) in BWRs or primary water chemistry in PWRs.

This report presents experimental data on crack growth rates (CGRs) of Types 304 and 316 SS irradiated up to 2.0 x 10^{21} n cm^{-2} (E > 1 MeV) at ≈288°C. The irradiations were carried out in a He environment in the Halden heavy water boiling reactor. Crack growth tests were conducted under cyclic loading with long rise times or constant load in normal water chemistry (NWC) and HWC BWR environments at 288°C.

EXPERIMENTAL

Crack growth tests have been conducted on Type 304 SS irradiated to 0.9 and 2.0 x 10^{21} n cm^{-2} (E > 1 MeV) (≈1.35 and 3.0 dpa) and on Type 316 SS irradiated to 2.0 x 10^{21} n cm^{-2} at ≈288°C. The tests were performed at ≈288°C on 1/4–T compact tension (CT) specimens in BWR environments. Figure 1 shows the configuration of the specimens. Crack extensions were determined by DC potential measurements.

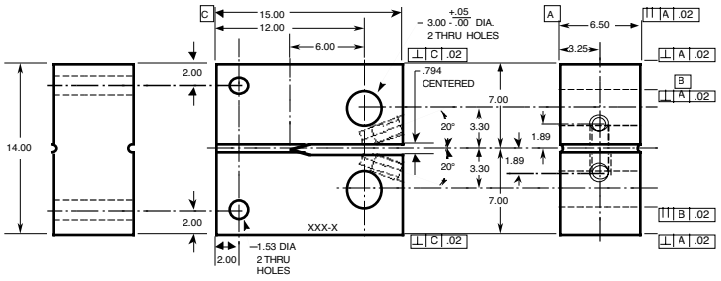

Figure 1. Configuration of compact–tension specimen for this study (dimensions in mm)

The facility for conducting the tests is designed for in–cell testing, with the test train, autoclave, and furnace mounted on top of a portable wheeled cart that can be easily rolled into the cell. The hydraulic actuator is mounted on top of the frame, with the test train components suspended beneath it. An Instron Model 8500+ Dynamic Materials Testing System is used for performing the tests. The load cage that contains the test specimen consists of the autoclave cover plate and a 12.7–mm bottom plate separated by four compression rods. The 1/4–T CT specimen is mounted between the actuator pull rod and the bottom plate of the load cage using a two–section clevis assembly. The top and bottom clevis assemblies are fastened with oxidized Zircaloy pins, electrically insulated with mica washers. Platinum wires are used for the current and potential leads. Water is circulated through a port in the autoclave cover plate that serves both as inlet and outlet.

The recirculating water system consists of a storage tank, high pressure pump, regenerative heat exchanger, autoclave preheater, test autoclave, electrochemical potential (ECP) cell preheater, ECP cell, regenerative heat exchanger, Mity Mite^{TM} back-pressure regulator, an ion–exchange cartridge, a 0.2 micron filter, a demineralizer resin bed, another 0.2 micron filter, and return line to the tank. A schematic diagram of the recirculating water system is shown in Fig. 2. Water is circulated at low flow rates, e.g., ≈10 mL/min.

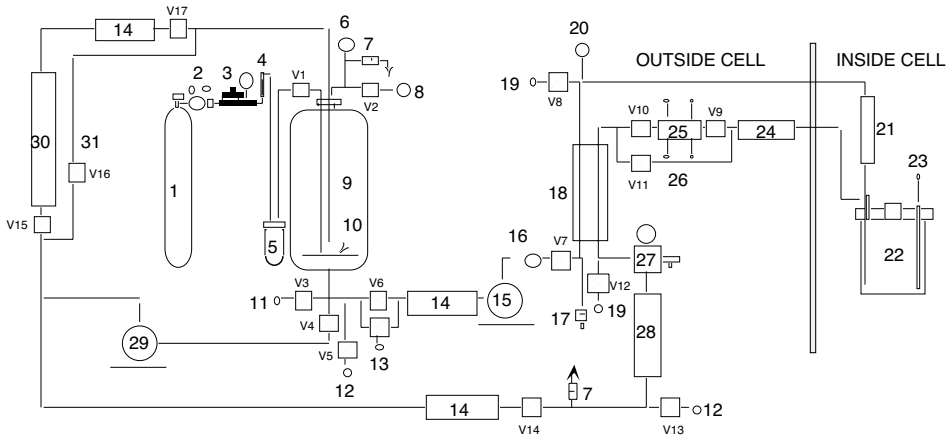

Figure 2. Schematic diagram of recirculating water system

The light water reactor (LWR) environments comprise high–purity–deionized water that contains either up to 300 ppb or <10 ppb dissolved oxygen (DO) to simulate NWC or HWC. The feedwater is stored in a 135–L SS tank. The tank is designed for vacuum and over–pressure to 60 psig. The deionized water is prepared by passing purified water through a set of filters that comprise a carbon filter, an Organex–Q filter, two ion exchangers, and a 0.2–mm

water is established by bubbling nitrogen that contains ≈1% oxygen through the deionized water. The DO is reduced to <10 ppb by bubbling nitrogen through the water; a vacuum is drawn on the tank cover gas to speed deoxygenation. The cover gas of the storage tank is nitrogen plus 1% oxygen for the high–DO environment and either pure nitrogen or nitrogen plus 5% hydrogen for the low–DO environment.

The CGR tests were performed in accordance with ASTM E–647 "Standard Test Method for Measurement of Fatigue Crack Growth Rates" and ASTM E–1681 "Standard Test Method for Determining a Threshold Stress Intensity Factor for Environment–Assisted Cracking of Metallic Materials under Constant Load." The composition of the SSs is presented in Table 1, and the tensile yield and ultimate stress for the steels irradiated to two fluence levels and in the nonirradiated condition [14,15] are given in Table 2.

Table 1. Composition (wt.%) of model austenitic stainless steels irradiated in the Halden reactor

Alloy ID[a]	Vendor Heat ID	Analysis	Ni	Si	P	S	Mn	C	N	Cr	Mo	O[b]
	Type 304 SS											
C3	PNL-C-6	Vendor	8.91	0.46	0.019	0.004	1.81	0.016	0.083	18.55		
		ANL	9.10	0.45	0.020	0.003	1.86	0.024	0.074	18.93		144
	Type 316 SS											
C16	PNL–SS–14	Vendor	12.90	0.38	0.014	0.002	1.66	0.020	0.011	16.92		–
		ANL	12.32	0.42	0.026	0.003	1.65	0.029	0.011	16.91	2.18	157

[a]First letters "C" and "L" denote commercial and laboratory heats, respectively.
[b]In wppm.

Table 2. Tensile properties[a] of irradiated austenitic stainless steels at 288°C

			Fluence (E > 1 MeV)			
	Nonirradiated		0.9 x 10^{21} n/cm^2		2.0 x 10^{21} n/cm^2	
Steel Type (Heat)	Yield (MPa)	Ultimate (MPa)	Yield (MPa)	Ultimate (MPa)	Yield (MPa)	Ultimate (MPa)
304 SS (C3)	(154)	(433)	632	668	796	826
316 SS (C16)	(189)	(483)	562	618	766	803

[a]Estimated values within parentheses.

All specimens were fatigue precracked in the environment at 288°C, triangular waveform, load ratio R = 0.2, and maximum stress intensity factor K_{max} ≈15 MPa m$^{1/2}$. After ≈0.5 mm crack advance, R was increased incrementally to 0.7, and the loading waveform changed to a slow/fast sawtooth with rise times of 30–1000 s. Constant load tests were conducted with the trapezoidal waveform, R = 0.7, 1–h hold period at peak, and 24–s unload/reload period. In both the cyclic and constant load tests, K_{max} was maintained approximately constant by periodic load shedding (less than 2% decrease in load at any given time). After the test the final crack size was marked by fatigue cycling at room temperature. The specimen was then fractured, and the fracture surface of both halves of the specimen was photographed through the cell window using a telephoto lens. The final crack length was measured from the photograph using the 9/8 averaging technique.

The CGR test results were validated in accordance with the specimen size criteria of ASTM E–1681 and E–647. To ensure that the experimental data obtained from different specimen geometry, thickness, and loading conditions can be compared with each other and applied to reactor components, the specimen size criteria require that the plastic zone at the tip of a fatigue crack be small relative to the specimen geometry. For constant load tests

$$B_{eff} \text{ and } (W–a) \geq 2.5\,(K/\sigma_{ys})^2 \quad (1)$$

and for cyclic loading

$$(W–a) \geq (4/\pi)\,(K/\sigma_{ys})^2, \quad (2)$$

where the effective specimen thickness B_{eff} is expressed in terms of the specimen thickness B and net specimen thickness B_N by the relationship $B_{eff} = (B\,B_N)^{0.5}$, W is the specimen width, a is the crack length, K is the applied stress intensity factor, and σ_{ys} is the yield stress of the material. In high–temperature water, because the primary mechanism for crack growth under cyclic loads with long rise times is not mechanical fatigue, Eq. 1 is probably more consistent with the ASTM Specifications for data qualification, but Eq. 2 may give acceptable results. The K/size criterion applies to work hardening materials and, therefore, breaks down markedly for materials irradiated to sufficient fluence such that on a local level, they do not strain harden. This lack of strain hardening or strain softening is most dramatic when dislocation channeling occurs but may also occur at lower fluences. For moderate to highly irradiated material, an effective yield stress defined as the average of the nonirradiated and irradiated yield stresses was used in the analysis. This discounts the irradiation–induced increase in yield strength by a factor of 2.

Crack growth tests have been completed at 289°C on 1/4–T CT specimens of Type 304 SS (Heat C3) irradiated to 0.9 and 2.0 x 10^{21} n·cm^{-2} and Type 316 SS (Heat C16) irradiated to 2.0 x 10^{21} n·cm^{-2}. The ECPs of a Pt electrode and SS electrode were monitored continuously during each test, while the water DO level and conductivity were determined periodically. Some significant results from these tests are presented below.

All tests were started in high–purity water containing 250–350 ppb DO (i.e., NWC BWR environment). After data were obtained for high–DO water, the DO level in the feedwater was decreased to <30 ppb by first sparging the feedwater with pure N_2 and then with N_2 + 5% H_2 (the latter simulates HWC). Because of the very low flow rates for the water system, it takes several days for the environmental conditions to stabilize. Changes in crack length and ECP of the Pt and SS electrodes during these transient periods are shown in Fig. 3 for specimen C3–B. The changes in steel ECP were slower than those in the Pt ECP. For example, although the Pt ECP decreased below –400 mV (SHE) within a couple of days, it took more than a week for the steel ECP to decrease below –400 mV.

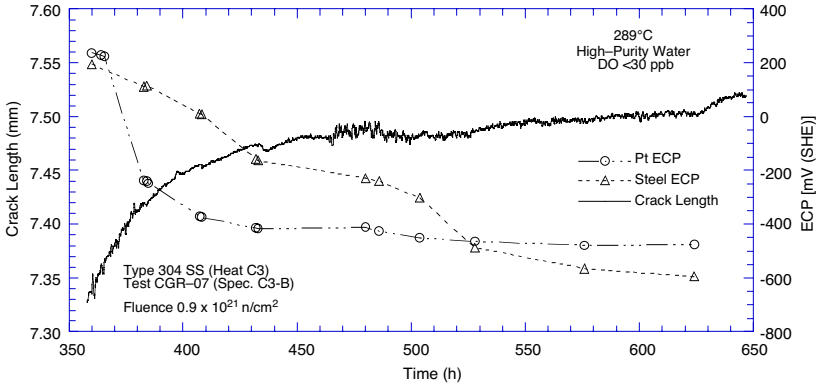

Figure 3. Change in crack length and ECP of Pt and SS electrodes for specimen C3–B after the DO level in the feedwater was decreased from ≈400 to <30 ppb

Under cyclic loading, the CGR (m/s) can be expressed as the superposition of the rate in air (i.e., mechanical fatigue) and the rates due to corrosion fatigue and SCC, given as

$$\dot{a}_{env} = \dot{a}_{air} + \dot{a}_{CF} + \dot{a}_{SCC}. \quad (3)$$

The results indicate that environmental enhancement of CGRs does not occur right from the start of the test. Under more rapid cyclic loading, the crack growth is dominated by mechanical fatigue. The CGRs during precracking and initial periods of cyclic loading were primarily due to mechanical fatigue. For the present tests on irradiated SSs, environmental enhancement typically was observed under loading conditions that would result in CGRs between 10^{-10} and 10^{-9} m/s in air. For K_{max} values of 15–18 MPa m$^{1/2}$ this corresponds to a load ratio R ≥ 0.5 and rise time ≥ 30 s. For specimen C3–B, environmental enhancement started after ≈170 h when the load ratio and rise time, respectively, were changed from 0.5 and 60 s to 0.7 and 300 s (Fig. 4). For the new loading condition, although the predicted CGR in air decreased by a factor of ≈15, the rate in water increased by a factor of ≈3.

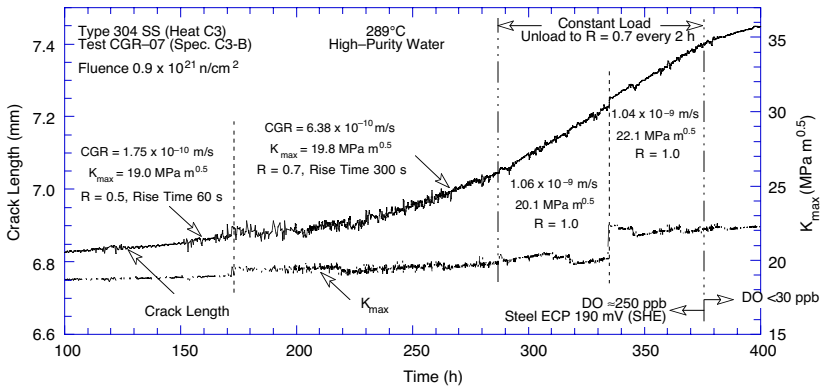

Figure 4. Crack–length–vs.–time plots for specimen C3–B in high–purity water at 289°C

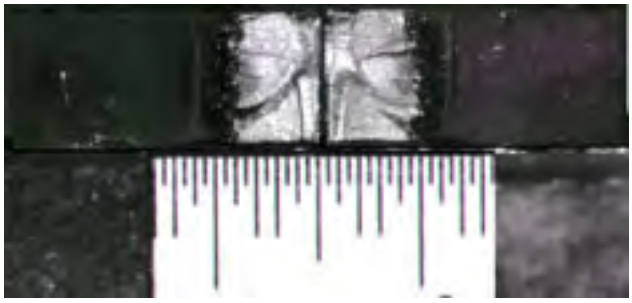

Figure 5. Photomicrographs of the fracture surface of specimen C3–B

For each test, the final crack length was measured from a photograph of the fracture surface (Fig. 5), and the results used to verify the data obtained from DC potential measurements. The difference in measured crack length and that estimated from the DC potential method was <5% for specimens C3–B and C16–B, and ≈40% for specimen C3–C. The large difference for specimen C3–C most likely was due to some unbroken ligaments observed on the fracture surface that provided additional conducting paths. For this test, the crack extensions estimated from the DC potential method were scaled proportionately to match the fractographic results.

In the present study, the K/size criterion of Eq. 1 was satisfied for all loading conditions for specimen C16–B and, as discussed later, all but one loading condition for specimen C3–C. For specimen C3–B, the applied K_{max} was slightly higher than that allowed by the K/size criterion; most results were obtained at an applied K_{max} of 22 MPa $m^{1/2}$. For these loading conditions the constant in Eq. 1 was 1.5 instead of 2.5.

For cyclic loading, the experimental CGRs for irradiated austenitic SSs in high– and low–DO environments and those predicted in air for the same loading conditions are plotted in Fig. 6. The curves represent the best–fit values for nonirradiated austenitic SSs in high–purity water with either 8 or 0.2 ppm DO [16]. The CGRs in air, $\dot{a}_{air}$ (m/s), were determined from the correlations developed by James and Jones [17]; the CGR is given by the expression

$$\dot{a}_{air} = C_{SS}\, S(R)\, \Delta K^{3.3}/t_R\,, \qquad (4)$$

where R is the load ratio (K_{min}/K_{max}), ΔK is $K_{max} - K_{min}$ in MPa $m^{1/2}$, t_R is the rise time (s) of the loading waveform, and the function S(R) is expressed in terms of the load ratio R as follows:

$$\begin{aligned} S(R) &= 1.0 && R < 0 \\ S(R) &= 1.0 + 1.8R && 0 < R < 0.79 \\ S(R) &= -43.35 + 57.97R && 0.79 < R < 1.0 \end{aligned} \qquad (5)$$

In addition, function C_{SS} is given by a third–order polynomial of temperature T (°C), expressed as

$$C_{SS} = 1.9142 \times 10^{-12} + 6.7911 \times 10^{-15}\, T - 1.6638 \times 10^{-17}\, T^2 + 3.9616 \times 10^{-20}\, T^3. \qquad (6)$$

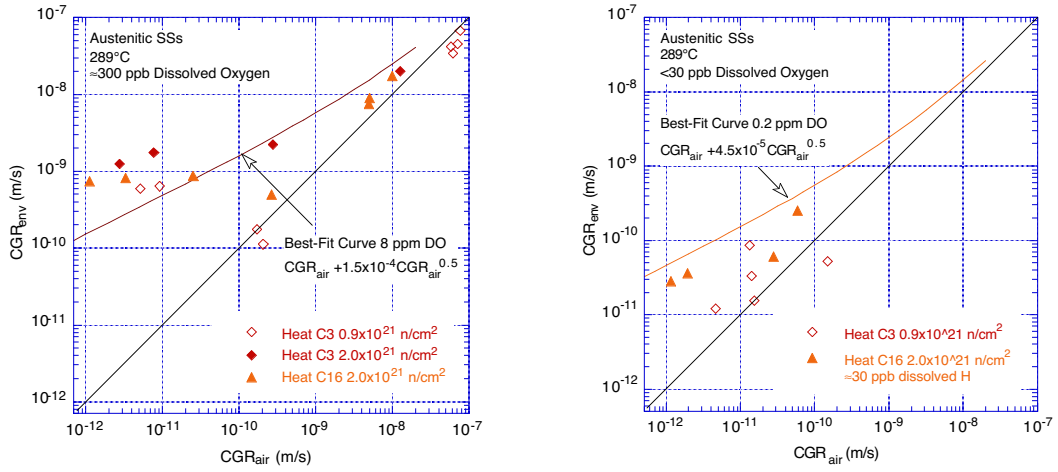

(a) (b)

Figure 6. CGR data for irradiated austenitic SSs under cyclic loading at 289°C in high–purity water with (a) ≈300 ppb and (b) <30 ppb dissolved oxygen.

The results indicate significant enhancement of CGRs of the irradiated steel in high–DO water (Fig. 6a) under cyclic loading with long rise times. The CGRs for Type 304 SS irradiated to either 0.9 or 2.0 x 10^{21} n·cm^{-2}, and Type 316 SS irradiated to 2.0 x 10^{21} n·cm^{-2} are comparable. In general, the CGRs for the irradiated steels in water with ≈ 300 ppb DO are slightly higher than for nonirradiated austenitic SSs in high–purity water with 8 ppm DO (Fig. 6a). For cyclic loading, decreasing the DO level has a beneficial effect on CGRs, e.g., the rates are decreased up to a factor of 25 in water with <30 ppb DO compared to those in water with ≈300 ppb DO. The growth rates for the irradiated steels in water with <30 ppb DO are slightly lower than for nonirradiated austenitic SSs in high–purity water with 0.2 ppm DO (Fig. 6b).

For constant load (i.e., a trapezoidal waveform), the experimental CGRs for irradiated SSs in high– and low–DO water are plotted in Fig. 7. In high–DO water, the CGRs obtained in the present study on Type 304 and 316 SS irradiated up to 2.0 x 10^{21} n·cm^{-2} are a factor of ≈5 higher than the disposition curve proposed in NUREG–0313 [18]. The growth rates for the two steels at the same fluence level, as well as for Type 304 SS irradiated to different fluence levels, are comparable. The results also indicate a benefit from a low–DO environment. For Heat C3 irradiated to 0.9 x 10^{21} n·cm^{-2} and Heat C16 irradiated to 2.0 x 10^{21} n·cm^{-2} (circles and diamonds in Fig. 7), the CGRs decreased more than an order of magnitude when the DO level was decreased from ≈300 ppb to <30 ppb.

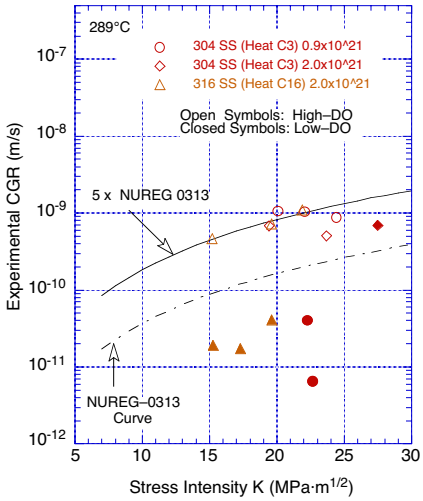

Figure 7.
Crack growth rate under constant load for irradiated austenitic SSs in high–purity water at 289°C

No benefit of low–DO environment was observed for Heat C3 irradiated to 2.0 x 10^{21} n·cm^{-2} (open and closed diamonds in Fig. 7), but the applied K_{max} for the test period in low–DO water was 44% greater than the allowable value based on the K/size criterion in Eq. 1. The crack length vs. time plot for the specimen during the decrease in DO level is shown in Fig. 8. No change in the slope of the curve is observed as the DO level was varied, but it is possible that the different behavior of C3–C is associated with the loss of constraint in the specimen due to the high applied load. Additional data are being obtained on Type 304 SS Heat C3 irradiated to 0.3 x 10^{21} n·cm^{-2} and Type 316 SS Heat C21 irradiated to 0.9 and 2.0 x 10^{21} n·cm^{-2}, to better establish the effect of decreased DO level on the CGRs of irradiated austenitic SSs.

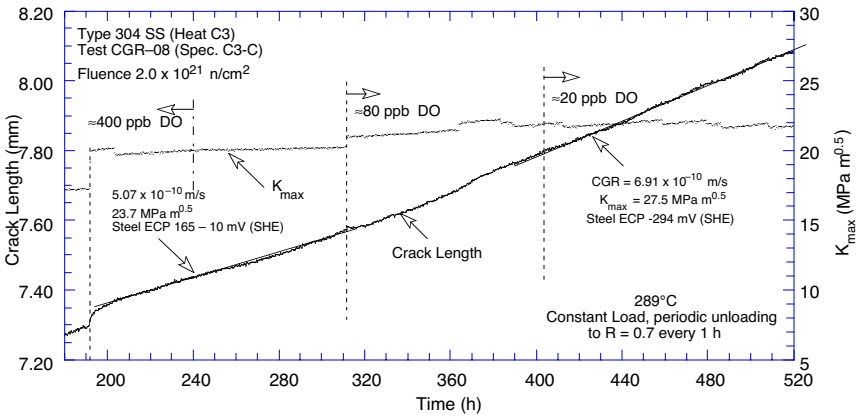

Figure 8. Crack–length–vs.–time plots for specimen C3–C in high–purity water at 289°C

CONCLUSIONS

Crack growth tests have been performed in BWR environments at ≈288°C on Type 304 SS (Heat C3) irradiated to 0.9 and 2.0 x 10^{21} n·cm^{-2} and Type 316 SS (Heat C16) irradiated to 2.0 x 10^{21} n·cm^{-2} at ≈288°C in a helium environment. Two waveforms were used in the tests, slow/fast sawtooth and trapezoidal. The cyclic loading was done with rise times between 30 and 1000 s. At the longer rise times, the environmental contributions to the crack growth rate dominate. The trapezoidal waveform essentially represents constant load with periodic unloading and loading. The results indicate significant enhancement of crack growth rates of the irradiated steel in the BWR environment with normal water chemistry. In the NWC BWR environment, the CGRs of irradiated steels are a factor of ≈5 higher than the disposition curve proposed in NUREG–0313 for nonirradiated austenitic SSs. The CGRs of Type 304 irradiated to 0.9 and 2.0 x 10^{21} n·cm^{-2} are comparable. The growth rates of irradiated Types 304 and 316 SS are also comparable.

In low–DO BWR environments, a decrease in the CGRs of the irradiated steels by an order of magnitude was observed in some tests. The beneficial effect of decreased DO was not observed for specimen C3–C irradiated to 2 x 10^{21} n·cm^{-2}. It is possible that the different behavior is associated with the loss of constraint in the specimen due to the high applied load. Additional data are being obtained on Type 304 SS (Heat C3) irradiated to 0.3 x 10^{21} n·cm^{-2} and Type 316 SS (Heat C21) irradiated to 0.9 and 2.0 x 10^{21} n·cm^{-2}.

ACKNOWLEDGMENTS

This work was sponsored by the Office of Nuclear Regulatory Research, U.S. Nuclear Regulatory Commission, FIN Number Y6388; Task Manager: C. Moyer; Program Manager: W. H. Cullen, Jr.

REFERENCES

1. Bruemmer, S. M., et al., *Critical Issue Reviews for the Understanding and Evaluation of Irradiation–Assisted Stress Corrosion Cracking*, EPRI TR–107159, Electric Power Research Institute, Palo Alto, CA, 1996.
2. Herrera, M. L., et al., "Evaluation of the Effects of Irradiation on the Fracture Toughness of BWR Internal Components," *Proc. ASME/JSME 4th Intl. Conf. on Nucl. Eng. (ICONE–4)*, Vol. 5, Eds., A. S. Rao, R. M. Duffey, and D. Elias, American Society of Mechanical Engineers, New York, pp. 245–251, 1996.
3. Mills, W. J., "Fracture Toughness of Type 304 and 316 Stainless Steels and their Welds," *Intl. Mater. Rev.,* 42, 1997, pp. 45–82.
4. Kanasaki, H., Satoh, I., Koyama, M., Okubo, T., Mager, T. R., and Lott, R. G., "Fatigue and Stress Corrosion Cracking Behaviors of Irradiated Stainless Steels in PWR Primary Water," *Proc. 5th Intl. Conf. on Nuclear Engineering,* ICONE5-2372, pp. 1–7, 1997.
5. Andresen, P. L., Ford, F. P., Murphy, S. M., and Perks, J. M., "State of Knowledge of Radiation Effects on Environmental Cracking in Light Water Reactor Core Materials, *Proc. 4th Intl. Symp. on Environmental Degradation of Materials in Nuclear Power Systems – Water Reactors,* NACE, pp. 1.83–1.121, 1990.
6. Jenssen, A. and Ljungberg, L. G., "Irradiation Assisted Stress Corrosion Cracking of Stainless Alloys in BWR Normal Water Chemistry and Hydrogen Water Chemistry," *Proc. Sixth Intl. Symp. on Environmental Degradation of Materials in Nuclear Power Systems – Water Reactor,* Eds., R. E. Gold and E. P. Simonen, The Minerals, Metals & Materials Society, pp. 547–553, 1993.
7. Gordon, G. M. and Brown, K. S., "Dependence of Creviced BWR Component IGSCC Behavior on Coolant Chemistry," *Proc. 4th Intl. Symp. on Environmental Degradation of Materials in Nuclear Power Systems – Water Reactor,* NACE, pp. 14.46–14.61, 1990.
8. Garzarolli, F., Alter, D., and Dewes, P., "Deformability of Austenitic Stainless Steels and Nickel–Base Alloys in the Core of a Boiling and a Pressurized Water Reactor," *Proc. Intl. Symp. on Environmental Degradation of Materials in Nuclear Power Systems – Water Reactor*, American Nuclear Society, pp. 131–138, 1986.
9. Kodama, M., et al., "IASCC Susceptibility of Austenitic Stainless Steels Irradiated to High Neutron Fluence, " *Proc. Sixth Intl. Symp. on Environmental Degradation of Materials in Nuclear Power Systems – Water Reactor,* Eds., R. E. Gold and E. P. Simonen, The Minerals, Metals & Materials Society, pp. 583–588, 1993.
10. Kodama, M., et al., "Effects of Fluence and Dissolved Oxygen on IASCC in Austenitic Stainless Steels, " *Proc. Fifth Intl. Symp. on Environmental Degradation of Materials in Nuclear Power Systems – Water Reactor,* American Nuclear Society, pp. 948–954, 1991.

11. Clark, W. L. and Jacobs, A. J., "Effect of Radiation Environment on SCC of Austenitic Materials," *Proc. First Intl. Symp. on Environmental Degradation of Materials in Nuclear Power Systems – Water Reactor*, NACE, pp. 451–461, 1983.
12. Jenssen, A. and Ljungberg, L. G., "Irradiation Assisted Stress Corrosion Cracking of Stainless Alloys in BWR Normal Water Chemistry and Hydrogen Water Chemistry," *Proc. Sixth Intl. Symp. on Environmental Degradation of Materials in Nuclear Power Systems – Water Reactor*, Eds., R. E. Gold and E. P. Simonen, The Minerals, Metals & Materials Society, pp. 547–553, 1993.
13. Jenssen, A. and Ljungberg, L. G., "Irradiation Assisted Stress Corrosion Cracking: Post Irradiation CERT Tests of Stainless Steels in a BWR Test Loop," *Proc. Seventh Intl. Symp. on Environmental Degradation of Materials in Nuclear Power Systems – Water Reactor*, Eds., G. Airey et al., NACE, pp. 1043–1052, 1995.
14. Chung, H. M., Ruther, W. E., Strain, R. V., and Shack, W. J., *Irradiated– Assisted Stress Corrosion Cracking of Model Austenitic Stainless Steel Alloys*, NUREG/CR–6687, ANL–00/21, Oct. 2000.
15. Chung, H. M., Strain, R. V., and Clark, R. W., "Slow–Strain–Rate–Tensile Test of Model Austenitic Stainless Steels Irradiated in the Halden Reactor," *Environmentally Assisted Cracking in Light Water Reactors Annual Report January–December 2001*, NUREG/CR–4667, Vol. 32, ANL–02/33, pp. 19–28, 2003.
16. Shack, W. J. and Kassner, T. F., "Review of Environmental Effects on Fatigue Crack Growth of Austenitic Stainless Steels," NUREG/CR–6176, ANL–94/1, May 1994.
17. James, L. A. and Jones, D. P., "Fatigue Crack Growth Correlation for Austenitic Stainless Steels in Air," *Proc. Conf. on Predictive Capabilities in Environmentally–Assisted Cracking*, PVP Vol. 99, Ed., R. Rungta, American Society of Mechanical Engineers, New York, pp. 363–414, 1985.
18. Hazelton, W. S. and Koo, W. H., *Technical Report on Material Selection and Processing Guidelines for BWR Coolant Pressure Boundary Piping, Final Report*, NUREG–0313, Rev. 2, Jan. 1988.